ARTICLES

Metal Carbonyl Cluster Synthesis in Nanocages: Spectroscopic Evidence of Intermediates in the Formation of $Ir_4(CO)_{12}$ in Zeolite NaY

Fen Li and Bruce C. Gates*

Department of Chemical Engineering and Materials Science, University of California, Davis, California 95616

Received: October 13, 2003; In Final Form: February 27, 2004

The assembly of $Ir_4(CO)_{12}$ from $Ir(CO)_2(acac)$ precursors in the supercages of zeolite NaY was investigated by extended X-ray absorption fine structure (EXAFS) and in-situ infrared (IR) spectroscopies. The data show that the conditions of pretreatment of the zeolite significantly affect the formation process of $Ir_4(CO)_{12}$. When the zeolite was initially largely dehydrated, so that the precursor molecules were well dispersed in the zeolite cages, dimeric intermediates in the formation of $Ir_4(CO)_{12}$ (approximated as $Ir_2(CO)_8$) were observed by both IR and EXAFS spectroscopies. In contrast, when the zeolite initially contained a substantial amount of water, the resultant Ir_4 clusters were formed faster than those in dehydrated zeolite, and evidence of intermediates was not observed. The results show how synthesis in the confined spaces of the zeolite nanopores—in the absence of solvents—affords opportunities to control and elucidate the chemistry, different from that in solution.

Introduction

Because the pores of faujasite zeolites are too small to allow entry of $Ir_4(CO)_{12}$, a ship-in-a-bottle synthesis method with the smaller precursor $Ir(CO)_2(acac)$ (acac is acetylacetonate) has been used to make this cluster in the supercages of zeolite NaY.[1,2] The chemistry of the intracage cluster assembly is less than well understood, but it is thought to be influenced by the concentration of water or OH groups in the zeolite, much as the comparable solution chemistry.[3] In an attempt to understand the intracage cluster synthesis better, we used zeolites pretreated under conditions to vary the water content and characterized the process of cluster formation using infrared (IR) spectroscopy to give evidence of the carbonyl ligands on the iridium and extended X-ray absorption fine structure (EXAFS) spectroscopy to provide evidence of Ir−Ir bonds in the iridium-containing species.

Experimental Methods

Materials. Zeolite NaY (obtained from the Davison Division of W. R. Grace) was treated either at about 25 °C under vacuum for 4 h (the sample is designated as zeolite NaY_{25}) or at 300 °C under a flow of O_2 for 4 h followed by vacuum for 12 h (giving zeolite NaY_{300}). Scanning electron microscope images of the zeolite, reported separately (with an image shown in Supporting Information),[4] show that the particles were highly crystalline and rather uniform in size, with an average diameter of about 0.5 μm.

Syntheses of metal clusters in the zeolites and sample transfers were performed with exclusion of air and moisture on a double-manifold Schlenk vacuum line and in a N_2-filled glovebox (AMO-2032, Vacuum Atmospheres). He and CO (99.995%) were purified by passage through traps containing particles of Cu and activated zeolite to remove traces of O_2 and moisture, respectively. *n*-Pentane (99.0% purity, Aldrich) and tetrahydrofuran (THF) (anhydrous, 99.9%, Aldrich), used as solvents, were refluxed under N_2 in the presence of Na/benzophenone ketyl to remove traces of water and then deoxygenated by sparging of dry N_2 prior to use. The precursor $Ir(CO)_2(acac)$ (dicarbonyl(acetylacetonato)iridium(I); 99%, Strem) and a compound used in extraction experiments, bis(triphenylphosphine)iminium chloride ([PPN][Cl]; 97%, Aldrich), were used as received.

Sample Preparation. $Ir(CO)_2(acac)$ dissolved in *n*-pentane was sorbed in the treated zeolite supports to give samples containing 1 wt % Ir after removal of the solvent (by evacuation at 25 °C). Carbonylation to form supported clusters was carried out with samples in flowing CO at 40 °C in a plug-flow reactor or in an IR cell set up as a flow reactor, as described elsewhere.[5,6]

Thermogravimetry (TG). The dehydration behavior of the zeolite support was investigated by thermogravimetric analysis linked with differential scanning calorimetry (TGA−DSC; the instrument was a Netzsch STA 449 C Jupiter). The zeolite sample described above (28.2 mg) was transferred under N_2 to the apparatus, (without evacuation) argon flow was started (at 40 mL/min), and the sample was heated at a rate of 10 °C/min as the sample mass and heat flow changes were recorded.

IR Spectroscopy. Spectra were recorded with a Bruker IFS-66v spectrometer with a spectral resolution of 4 cm^{-1}. Samples in the glovebox were pressed into thin self-supporting wafers and mounted in a controlled-atmosphere IR cell. Each sample was scanned as purified He or CO flowed through the cell. Each spectrum is the average of 64 scans. Details of the experiments are as reported elsewhere.[6]

Attempted Extraction of Metal Carbonyls from Zeolite NaY. Attempts were made to extract iridium carbonyls from the zeolite by bringing the samples in contact with [PPN][Cl] in freshly distilled THF under N_2. The supernatant liquid was transferred by syringe into a solution IR cell and quickly scanned. In earlier work, successful extractions of $Ir_4(CO)_{12}$ and

10.1021/jp037100m CCC: $27.50
Published on Web 07/03/2004

TABLE 1: Crystallographic Data Characterizing the Reference Compounds and Fourier Transform Ranges Used in the EXAFS Data Analysis[a]

	crystallographic data			Fourier transform		
sample	shell	N	R (Å)	Δk (Å^{-1})	Δr (Å)	n
Ir crystal	Ir−Ir[b]	12	2.72	0.9−19.4	1.6−3.3	1
$Na_2Pt(OH)_6$	Pt−O[c]	6	2.05	1.4−17.7	0.5−2.0	3
$Ir_4(CO)_{12}$	Ir−C[d]	3	1.87	2.8−16.5	1.1−2.0	3
	Ir−O*[d]	3	3.01	2.8−16.5	2.0−3.3	3

[a] Notation: N, coordination number for the absorber−backscatterer pair; R, distance; Δk, limits used for the forward Fourier transform (k is the wave vector); Δr, limits used for shell isolation (r is distance); n, power of k used for the Fourier transformation. [b] Crystal structure data from ref 12. [c] Crystal structure data from ref 13. [d] Crystal structure data from ref 15.

of $Ir_6(CO)_{16}$ from γ-Al_2O_3 have been carried out.[7,8] Unsuccessful attempts to extract these clusters from faujasite zeolites have been taken as evidence of entrapment of the clusters in the zeolite supercages.[6,9]

X-ray Absorption Spectroscopy. EXAFS spectroscopy experiments were performed at X-ray beamline X-11A at the National Synchrotron Light Source at Brookhaven National Laboratory (BNL), Upton, NY. The storage ring energy was 2.8 GeV, and the ring current was 180−280 mA. The EXAFS data were recorded in the transmission mode after the cells had been cooled to nearly liquid nitrogen temperature. Each sample was scanned several times, and the typical spectrum is the average of four scans, although occasionally there were fewer. The data were collected with a Si(111) double-crystal monochromator that was detuned by 30% to minimize effects of higher harmonics in the X-ray beam. The samples were scanned at energies near the Ir L_{III} absorption edge (11215 eV). Details are as reported elsewhere.[5,9,10]

Analysis of EXAFS Data. The methods of EXAFS data analysis are essentially the same as those described elsewhere.[11] The data were analyzed with experimentally determined reference files obtained from EXAFS data characterizing materials of known structure, but the Ir−Ir reference file was calculated theoretically with the software FEFF-7.[12] The Ir−O support interaction was analyzed with phase shifts and backscattering amplitudes obtained from data characterizing the reference compound $Na_2Pt(OH)_6$;[13] the transferability of the phase shifts and backscattering amplitudes characterizing platinum and iridium (which are near neighbors in the periodic table) has been justified experimentally.[14] The Ir−C and Ir−O* contributions (where O* represents carbonyl oxygen) were analyzed with phase shifts and backscattering amplitudes obtained from EXAFS data characterizing the crystalline reference compound $Ir_4(CO)_{12}$, which has terminal CO ligands.[15]

The parameters used in the analysis of the EXAFS data characterizing the zeolite-supported samples are summarized in Table 1. The parameters representing the high-Z (Ir−Ir) and low-Z (Ir−$O_{support}$, Ir−CO) contributions were determined by multiple-shell fitting in both r (distance) and k (wave vector) space with comparisons of data and fits for both k^1 and k^3 weightings.[16] The data quality is high, and the analysis was carried out without Fourier filtering, as described elsewhere.[17]

Results

TG Characterization of the Zeolite Support. The thermogravimetric analysis results characterizing the support are presented in the Supporting Information. The data show that the water contents of zeolite NaY_{300} and NaY_{25} were about 1 and 24 wt %, respectively. Almost all the water had been removed when the temperature reached about 600 °C.

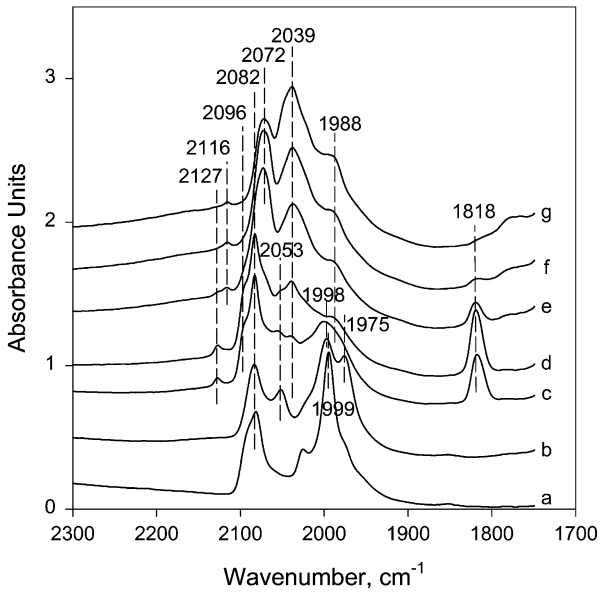

Figure 1. IR spectra characterizing the carbonylation of $Ir(CO)_2(acac)$ sorbed in zeolite NaY_{300}: (a) sample after evacuation for 2 days at 25 °C; (b) sample treated in He at 40 °C, and then treated in CO at 40 °C for (c) 5 min, (d) 30 min, (e) 2 h, (f) 4 h, and (g) 20 h.

Process of Formation of $Ir_4(CO)_{12}$ in Zeolite NaY_{300}. *IR Evidence.* After zeolite NaY_{300} had been brought into contact with $Ir(CO)_2(acac)$ in *n*-pentane solution and the solvent removed by evacuation for 2 days, the solid was light beige in color and had an IR spectrum with two strong ν_{CO} bands, at 2082 and 1999 cm^{-1} (Figure 1a), indicating a mononuclear iridium dicarbonyl species.[6] After treatment of this sample in flowing He at 40 °C, two new ν_{CO} bands appeared, at 2053 and 1975 cm^{-1} (Figure 1b). Then after flow of CO at 40 °C for 5 min, three additional new ν_{CO} bands appeared, at 2127, 2039, and 1818 cm^{-1}, and a new shoulder appeared at 2096 cm^{-1} (Figure 1c). The band at 1818 cm^{-1} represents edge-bridging CO ligands[18] and suggests the formation of Ir−Ir bonds. During CO treatment, the band at 1975 cm^{-1} appeared to shift to higher frequency, so that the band at 1998 cm^{-1} appeared broadened, with a shoulder (Figure 1c). After 30 min of CO treatment at 40 °C, the ν_{CO} bands at 2127, 2096, 2082, 2053, 2039, and 1818 cm^{-1} had increased in intensity, and the ν_{CO} band at 1998 cm^{-1} had decreased in intensity and become a shoulder at about 1988 cm^{-1} (Figure 1d).

After treatment of this sample in flowing CO at 40 °C for longer periods, the ν_{CO} bands at 2116 and 2039 cm^{-1} had increased in intensity, a band at 2072 cm^{-1} grew in, and the bands at 2127 and 1818 cm^{-1} decreased gradually during the continued treatment until they disappeared after 20 h (Figure 1). The final spectrum (Figure 1g) essentially matches that attributed to $Ir_4(CO)_{12}$ in zeolite NaY;[6] this cluster is highly carbonylated, and all the CO ligands are terminal. The changes in the spectrum are inferred to be indicative of intermediate species formed during the carbonylation treatment to form $Ir_4(CO)_{12}$.

Attempts to extract this iridium carbonyl cluster from zeolite NaY_{300} with [PPN][Cl] in THF were not successful (although $Ir_4(CO)_{12}$ is slightly soluble in THF, and even more soluble in [PPN][Cl]/THF mixtures). The supernatant solution had no IR absorptions in the ν_{CO} region. This result is consistent with that of previous work[6] and with the entrapment of iridium carbonyl clusters in the zeolite cages (the approximate diameter of Ir_4-

$(CO)_{12}$ is 9 Å, that of the zeolite supercage is 12.5 Å, and that of the apertures connecting the supercages is 7.4 Å).

EXAFS Evidence. EXAFS data reported earlier[4] show that more than 4 h of CO treatment at 40 °C of $Ir(CO)_2(acac)$ sorbed in zeolite NaY_{300} led to the formation of zeolite-supported $Ir_4(CO)_{12}$, consistent with the IR spectrum of Figure 1g.

In an attempt to prepare a sample containing intermediates en route to the formation of $Ir_4(CO)_{12}$ for EXAFS characterization, the $Ir(CO)_2(acac)$-containing zeolite NaY_{300} sample was treated under carbonylation conditions at 40 °C in a plug-flow reactor. After treatment for 30 min, the sample was taken out of the reactor and mixed thoroughly. Part of the sample was used to prepare a wafer for IR spectroscopy.

The IR spectrum of the sample was found to be almost the same as that of Figure 1a, indicating no significant changes after this short period of carbonylation. Because the carbonylation process was carried out in a plug-flow reactor, we infer that it was slower than that described above for the thin self-supporting wafer in the IR cell, presumably because of mass-transfer and mixing effects. (The pattern is suggestive of differences between deep bed and shallow bed treatments of zeolites, for example, calcinations.[19]) Consequently, carbonylations in the fixed-bed reactor were carried out for various times (1, 1.5, and 2 h), and the IR spectra were checked, as before. After 2.5 h of treatment, the IR spectrum was almost the same as that of Figure 1d.

The EXAFS data at the Ir L_{III} edge characterizing this sample are shown in Figure 2, with the parameters determined by the data fitting summarized in Table 2. The data show oscillations up to a value of k of about 16 $Å^{-1}$, indicating the presence of near-neighbor high-atomic-weight scatterers in the near vicinity of the Ir atoms. There was no evidence in the Fourier transform of second- or higher-shell Ir−Ir contributions.

The software XDAP[20,21] was used to estimate the errors shown in Table 2; these represent precisions, not accuracies. The accuracies are estimated to be as follows: coordination number (N), Ir−Ir, ±20%, and Ir−$O_{support}$, ±30%; distance (R), Ir−Ir, ±1%, and Ir−C and Ir−O, ±2%; Debye−Waller factor ($\Delta\sigma^2$), ±30%; inner potential correction (ΔE_0), ±10%. The number of parameters used to fit the data in this main shell analysis, n, was 20; the statistically justified number is approximately 42, estimated from the Nyquist theorem,[22] $n = (2\Delta k\Delta r/\pi) + 1$, where Δk and Δr, respectively, are the k and r ranges used in the forward and inverse Fourier transforms ($\Delta k = 13.0$ $Å^{-1}$, $\Delta r = 5$ Å).

The EXAFS data are inferred to characterize intermediates in the formation process of $Ir_4(CO)_{12}$ in zeolite NaY_{300}. They indicate an Ir−Ir coordination number of 0.9 (at an average distance of 2.69 Å) and thus provide evidence of the formation of Ir−Ir bonds from the precursors. The Ir−C_t and Ir− C_b (the subscripts t and b refer to terminal and bridging, respectively) coordination numbers were found to be 1.2 and 2.0, respectively, with distances of 1.76 and 1.88 Å, respectively; the Ir−O* coordination number was found to be 2.6, at an average distance of 2.92 Å (the uncertainty in these parameters is higher than the values stated above because mixtures of terminal and bridging ligands are difficult to resolve).

These results indicate that, on average, the mononuclear precursor was converted into dimeric iridium carbonyls, which are inferred to be intermediates in the formation of zeolite NaY_{300}-supported $Ir_4(CO)_{12}$. The data are consistent with the IR results that indicate the formation of Ir−Ir bonds in intermediates en route to $Ir_4(CO)_{12}$.

Process of Formation of $Ir_4(CO)_{12}$ in Zeolite NaY_{25}. *IR Evidence.* Zeolite NaY_{25} was held in contact with $Ir(CO)_2(acac)$ in *n*-pentane solution for 2 days. After removal of the solvent by evacuation for 2 days, the solid was beige in color and had an IR spectrum with two strong ν_{CO} bands, at 2080 and 2000 cm^{-1} (Figure 3a), indicating an iridium dicarbonyl species.[6] Upon treatment of this sample in flowing He at 40 °C, these two ν_{CO} bands became broadened (Figure 3b), suggesting the appearance of new ν_{CO} bands nearby. Then after CO had flowed over the sample at 40 °C for only 1 min, a new IR spectrum emerged; the ν_{CO} band at 2080 cm^{-1} shifted to lower frequency (2072 cm^{-1}), and those near 2000 cm^{-1} shifted to higher frequencies (Figure 3c). After 5 min of CO flow, a new ν_{CO} band appeared at 2116 cm^{-1}, and the band located near 2000 cm^{-1} shifted to higher energy (2034 cm^{-1}, Figure 3d). After continued treatment of this sample in flowing CO at 40 °C for 8 h, a light-brown-colored solid formed, with the IR spectrum

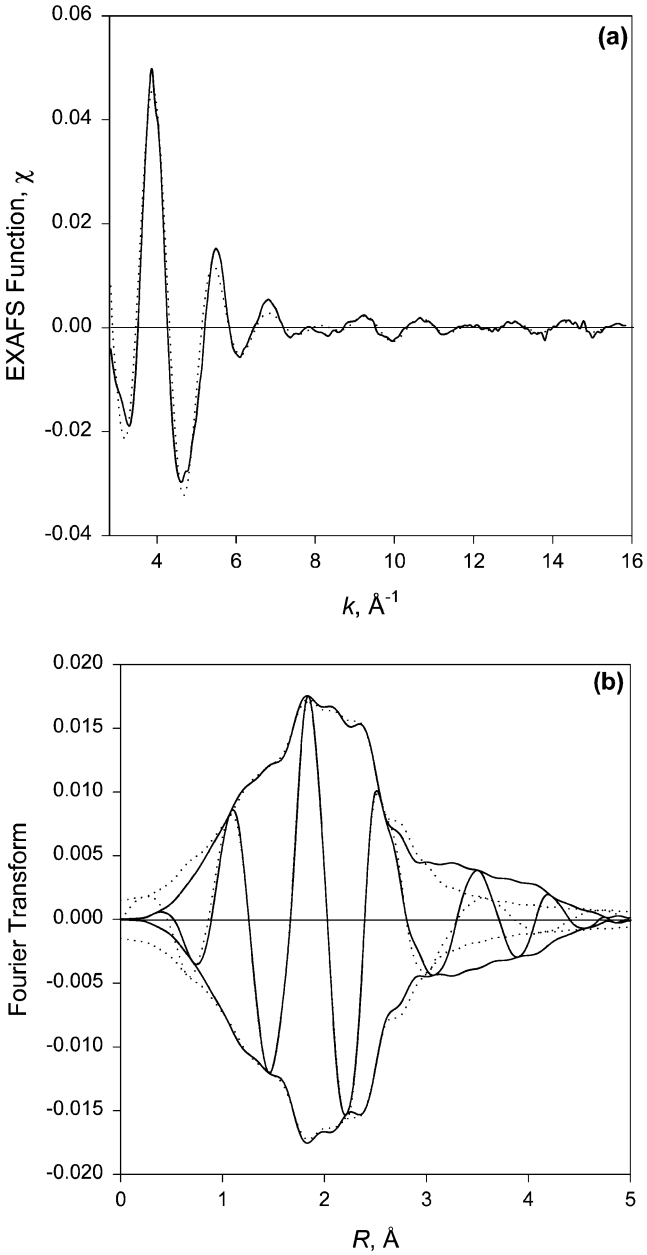

Figure 2. Results of EXAFS analysis characterizing products during the carbonylation of $Ir(CO)_2(acac)$ sorbed in zeolite NaY_{300} (treatment: CO, 40 °C for 2.5 h): (a) experimental EXAFS (χ) function (solid line) and the sum of the calculated contributions (dotted line); (b) imaginary part and magnitude of the uncorrected Fourier transform (k^0 weighted, $\Delta k = 2.8-15.8$ $Å^{-1}$) of experimental EXAFS (solid line) and sum of the calculated contributions (dotted line).

TABLE 2: EXAFS Results Characterizing CO Treatment of $Ir(CO)_2(acac)$ Sorbed in Zeolite NaY_{300} at 40 °C for 2.5 h[a]

	EXAFS parameters				
shell	N	R (Å)	$10^3\Delta\sigma^2$ (Å^2)	ΔE_0 (eV)	EXAFS ref
Ir−Ir	0.9 ± 0.1	2.69 ± 0.01	3.5 ± 0.8	1.6 ± 1.4	Ir−Ir
Ir−O_s	1.8 ± 0.1	2.11 ± 0.01	0.8 ± 0.5	2.0 ± 0.5	Pt−O
Ir−CO					
Ir−C_t	1.2 ± 0.2	1.76 ± 0.03	3.6 ± 1.8	−2.1 ± 1.1	Ir−C
Ir−C_b	2.0 ± 0.1	1.88 ± 0.01	2.0 ± 1.4	1.0 ± 0.7	Ir−C
Ir−O*	2.6 ± 0.1	2.92 ± 0.01	10.0 ± 1.1	2.5 ± 0.4	Ir−O*

[a] Notation: N, coordination number; R, distance between absorber and backscatterer atoms; $\Delta\sigma^2$, Debye−Waller factor; ΔE_0, inner potential correction; the subscripts s, t, and b refer to short, terminal, and bridging, respectively.

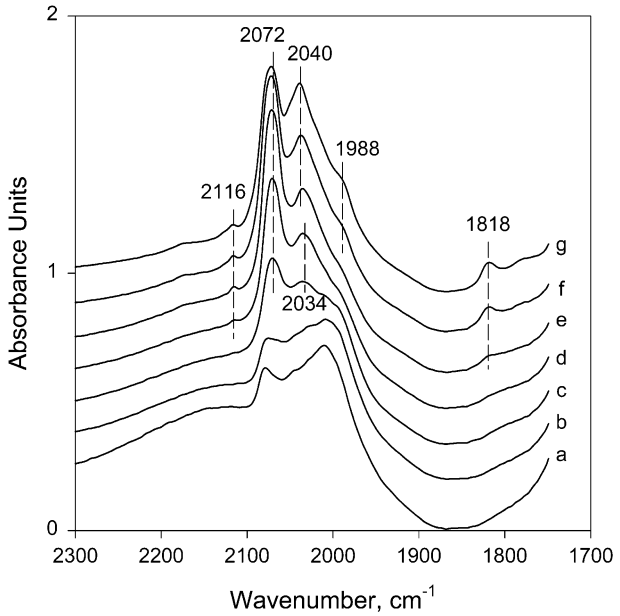

Figure 3. IR spectra characterizing the carbonylation of $Ir(CO)_2(acac)$ sorbed in zeolite NaY_{25}: (a) sample after evacuation for 2 days at 25 °C; (b) sample treated in He at 40 °C, and then treated in CO at 40 °C for (c) 1 min, (d) 5 min, (e) 1 h, (f) 8 h, and (g) 20 h.

shown in Figure 3f (ν_{CO} = 2116, 2072, and 2040 cm^{-1}). The spectrum remained unchanged after 20 h of treatment in CO (Figure 3g), and it closely resembles that attributed to $Ir_4(CO)_{12}$ supported on zeolite NaY.[6,23,24]

Attempts to extract this iridium carbonyl from the zeolite with [PPN][Cl] in THF were not successful, consistent with the formation of clusters trapped in the zeolite cages.

A comparison of the IR spectra of the samples supported on zeolites NaY_{300} and NaY_{25} shows differences in the cluster formation process: the spectra of the iridium carbonyls in zeolite NaY_{300} include some ν_{CO} bands that grew in and then disappeared, indicating the appearance of intermediates; in contrast, the IR spectra characterizing the sample supported on zeolite NaY_{25} include no evidence of such intermediates, as all the new bands that formed increased gradually in intensity.

EXAFS Evidence. Previous EXAFS work also showed that more than 4 h of CO treatment at 40 °C of $Ir(CO)_2(acac)$ sorbed in zeolite NaY_{25} led to the formation of $Ir_4(CO)_{12}$, corresponding to the IR spectrum of Figure 3g (except for the peak at 1818 cm^{-1}, which is discussed below). To compare what was present during the $Ir_4(CO)_{12}$ formation process in zeolite NaY_{25} with what was present in zeolite NaY_{300}, the zeolite NaY_{25}-supported sample after carbonylation under the same conditions and for the same time (2.5 h) (which was characterized by an IR spectrum essentially the same as that of Figure 3d) was characterized by EXAFS spectroscopy.

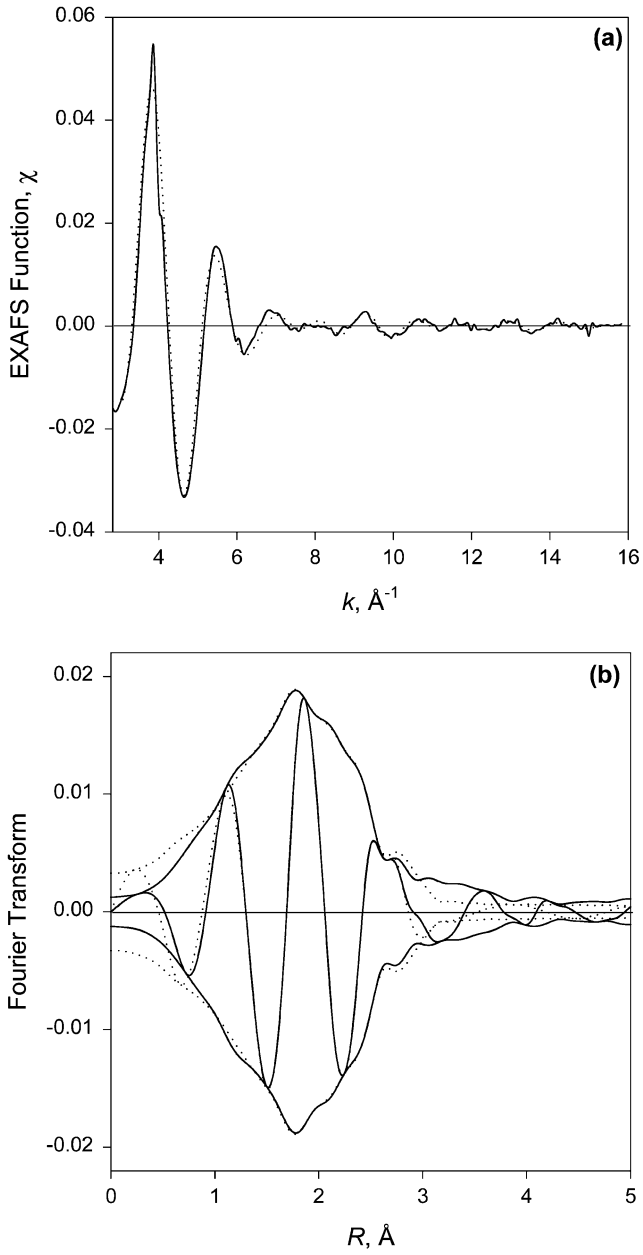

Figure 4. Results of EXAFS analysis characterizing products during the carbonylation of $Ir(CO)_2(acac)$ sorbed in zeolite NaY_{25} (treatment: CO, 40 °C for 2.5 h): (a) experimental EXAFS (χ) function (solid line) and the sum of the calculated contributions (dotted line); (b) imaginary part and magnitude of the uncorrected Fourier transform (k^0 weighted, Δk = 2.8−15.8 Å^{-1}) of experimental EXAFS (solid line) and sum of the calculated contributions (dotted line).

The EXAFS data at the Ir L_{III} edge characterizing this sample are shown in Figure 4, and the parameters determined by the data fitting are summarized in Table 3. The data show oscillations up to a value of k of about 15 Å^{-1}, indicating the presence of near-neighbor high-atomic-weight scatterers. There was no evidence in the Fourier transform of second- or higher-shell Ir−Ir contributions. The number of parameters used to fit the data in this main shell analysis, n, was 16; the statistically justified number is approximately 42.

These EXAFS data characterizing the sample en route to the formation of $Ir_4(CO)_{12}$ in zeolite NaY_{25} (Table 3) indicate an Ir−Ir coordination number of 2.4, at an average distance of 2.71 Å; the Ir−C_t and Ir−O* coordination numbers were found to

TABLE 3: EXAFS Results Characterizing CO Treatment of $Ir(CO)_2(acac)$ Sorbed in Zeolite NaY_{25} at 40 °C for 2.5 h[a]

shell	EXAFS parameters				EXAFS ref
	N	R (Å)	$10^3\Delta\sigma^2$ (Å^2)	ΔE_0 (eV)	
Ir−Ir	2.4 ± 0.1	2.71 ± 0.01	5.9 ± 0.5	−1.7 ± 0.6	Ir−Ir
Ir−O_s	1.5 ± 0.1	2.11 ± 0.01	0.7 ± 0.7	−2.0 ± 0.4	Pt−O
Ir−CO					
Ir−C_t	1.5 ± 0.1	1.85 ± 0.01	5.0 ± 1.2	0.0 ± 0.6	Ir−C
Ir−O*	1.0 ± 0.1	2.97 ± 0.01	0.8 ± 0.8	0.6 ± 0.5	Ir−O*

[a] Notation as in Table 2.

be 1.5 and 1.0, respectively, with distances of 1.85 and 2.97 Å, respectively. The crystallographic data representing $Ir_4(CO)_{12}$[15] show that each Ir atom in the cluster in the crystalline state is bonded to three other Ir atoms (the coordination number is 3), at an average distance of 2.69 Å; each Ir atom also has three terminal carbonyl ligands, at an average Ir−C distance of 1.87 Å and an Ir−O* distance of 3.01 Å. Thus, the data indicate that the precursor $Ir(CO)_2(acac)$ at this stage of transformation had formed iridium carbonyl clusters with average properties that match, within the expected errors, those of $Ir_4(CO)_{12}$.

Thus, the IR and EXAFS results characterizing the sample carbonylated in zeolite NaY_{25} give clear evidence of the formation of $Ir_4(CO)_{12}$, but not of intermediates in the cluster formation, in contrast to the observations characterizing the iridium carbonyls in zeolite NaY_{300}.

Discussion

The contrasting results obtained with zeolite NaY_{300} and zeolite NaY_{25} indicate an effect of the zeolite water content on the process of intracage cluster formation, although the final carbonylation product, $Ir_4(CO)_{12}$, was essentially the same in each zeolite. In contrast, both IR and EXAFS data reported earlier[4,6] show that the decarbonylation of $Ir_4(CO)_{12}$/zeolite NaY to form Ir_4/zeolite NaY and the reversible recarbonylation to give back $Ir_4(CO)_{12}$/zeolite NaY were not affected substantially by the initial pretreatment of the zeolite, at least under the conditions of the reported experiments (CO, 40 °C).

According to the TG result, zeolite NaY_{300} was almost completely dehydrated, with almost all of the supercages available for sorption of the precursor $Ir(CO)_2(acac)$. Because the $Ir(CO)_2(acac)$/supercage ratio used in the preparation was only about 1/12, the $Ir(CO)_2(acac)$ precursors are inferred to have been well separated and largely isolated from each other in the zeolite cages. When subjected to carbonylation conditions, the precursors and/or intermediates in zeolite NaY_{300} evidently migrated between cages and, over a period of hours at 40 °C, formed $Ir_4(CO)_{12}$. (There is strong evidence for migration of such species on oxide surfaces and in zeolites.[25]) The IR spectra (Figure 1c−e) show the presence of bridging CO ligands (which implies the presence of Ir−Ir bonds) increasing in the beginning, then decreasing, and disappearing, and correspondingly, the EXAFS results indicate the presence of small intermediates, on average approximately diiridium carbonyl species (the Ir−Ir coordination number was approximately 1). Thus, both the IR and EXAFS results indicate the presence in zeolite NaY_{300} of intermediates larger than the mononuclear precursors and smaller than the clusters that were finally formed.

In contrast, zeolite NaY_{25} was only slightly dehydrated. (Before evacuation, zeolite NaY typically contains about 26 wt % water at room temperature,[26] and so our data show that only a few percent of the water had been removed from zeolite NaY_{25}.) The results of the attempted extraction of metal carbonyls from both zeolites show that the iridium carbonyl clusters were trapped in the zeolite cages. We suggest that it was principally supercages near the external surfaces of the zeolite NaY_{25} crystallites that were accessible to the $Ir(CO)_2$-(acac) precursors, as the pores were largely filled with water. If these precursors were concentrated in the cages near the zeolite NaY_{25} crystallite surfaces, then the precursors would have been present nearer to each other than those in zeolite NaY_{300}, facilitating their reaction with each other to form clusters. This hypothesis would account for the observation that the assembly of $Ir_4(CO)_{12}$ took place more rapidly during carbonylation in zeolite NaY_{25} than in zeolite NaY_{300}, without evidence of intermediates in the former.

The results presented here may be compared with those of the solution chemistry of the formation of $Ir_4(CO)_2$ from iridium salts developed by Pergola et al.:[27]

$$IrCl_3 + 3CO + H_2O \rightarrow [Ir(CO)_2Cl_2]^- + Cl^- + 2H^+ + CO_2 \quad (1)$$

$$4[Ir(CO)_2Cl_2]^- + 6CO + 2H_2O \rightarrow Ir_4(CO)_{12} + 2CO_2 + 4H^+ + 8Cl^- \quad (2)$$

Both synthesis in the zeolites and synthesis in solution take place in the presence of CO under mild conditions: in the zeolites at 40 °C and in solution at 110 °C for step 1 and 25 °C for step 2. Because both zeolite NaY_{300} and zeolite NaY_{25} contained water, we infer that water plays a role in the synthesis in the zeolites, as it does in solution. Beneke et al.[3b] investigated the effect of zeolite water in the carbonylation of Pt(II) to make platinum clusters in zeolite NaX. Their in situ FTIR and UV−vis spectroscopy results showed that water accelerated the carbonylation process.

The IR spectra (Figure 1c−e) characterizing the formation of $Ir_4(CO)_{12}$ in zeolite NaY_{300} show intermediate species with ν_{CO} bands at 2127, 2096, 2082, 2053, 2039, 1988 sh, and 1818 cm^{-1}. (The 1818 cm^{-1} band might suggest the isomer of Ir_6-$(CO)_{16}$ that has edge-bridging CO ligands,[5,28] but the difference is that the bands at 2039 and 1818 cm^{-1} of Figure 1d are much less intense than those of $Ir_6(CO)_{16}$, and there is a shoulder at 1988 cm^{-1} in Figure 1d.) For comparison, the spectrum of bridge-bonded $Ir_2(CO)_8$ is characterized by ν_{CO} bands at 2095 ms, 2060 s br, 1848 w sh, and 1822 m cm^{-1},[18] and that of the isomer of $Ir_2(CO)_8$ without bridge-bonded CO is characterized by ν_{CO} bands at 2062, 2055, and 2040 cm^{-1}.[29] There are four ν_{CO} bands characterizing our zeolite-supported intermediate species (2096, 2053, 2039, and 1818 cm^{-1}) that essentially match bands of $Ir_2(CO)_8$. Thus, we suggest that $Ir_2(CO)_8$ itself was present in zeolite NaY_{300} during the CO-induced formation of $Ir_4(CO)_{12}$ at 40 °C.

In an investigation of the solution synthesis of $Ir_4(CO)_{12}$ reported by Whyman,[30] IR evidence was found for $HIr(CO)_4$ but not $Ir_2(CO)_8$, in contrast to the results obtained for the corresponding synthesis of carbonyls of cobalt and of rhodium, which indicate that an equilibrium is attained:[31,32]

$$M_4(CO)_{12} + 4CO \rightleftarrows 2M_2(CO)_8 \quad (3)$$

where M = Co or Rh.

However, investigation of the synthesis of $Ir_4(CO)_{12}$ in a CO matrix at −258 °C gave evidence of $Ir_2(CO)_8$.[18] Under the low-temperature conditions of this experiment, the cluster formation was evidently slow enough for observations of the intermediate, as it was in zeolite NaY_{300}. The slowness of the cluster formation in zeolite NaY_{300} may be attributed to some combination of

the effects of low water concentration, wide spacing of the iridium precursors, and slow migration of these precursors in the zeolite pores.

There are few examples of intermediates in the formation of metal cluster compounds, and the results presented here may be the first characterizing such intermediates in a solid phase when the temperature was not extremely low.

Control of the location of the metal clusters within zeolite crystals is important in catalyst design, as it is usually desirable to make all the clusters accessible to reactants. Our data suggest that the clusters formed in the zeolite initially containing a substantial amount of water were concentrated near the external surface of the zeolite crystals; if this suggestion is correct, then the preparation with the zeolite containing a large amount of water would be expected to give clusters concentrated near the pore mouths of the zeolite, which would offer the advantage of accessibility to reactant molecules in catalysis of reactions affected by intracrystalline mass transfer.

Conclusions

The water content of zeolite NaY supports affects the rate of formation of $Ir_4(CO)_{12}$ from $Ir(CO)_2(acac)$ in the zeolite cages. $Ir_4(CO)_{12}$ formed more slowly in zeolite NaY_{300} than in zeolite NaY_{25}, and both IR and EXAFS data gave evidence of intermediates in the carbonylation process in zeolite NaY_{300}. The spectra are consistent with the identification of $Ir_2(CO)_8$ as an intermediate in the cluster formation in zeolite NaY_{300}.

Acknowledgment. This research was supported by the U.S. Department of Energy, Office of Energy Research, Office of Basic Energy Sciences, Division of Chemical Sciences, Contract No. FG02-87ER13790. EXAFS experiments were done at the NSLS (beam line X-11A), which is operated by the Department of Energy, Office of Basic Energy Sciences. The NSLS is supported by the Department of Energy, Division of Materials Sciences and Division of Chemical Sciences, under Contract No. DE-AC02-76CH00016. We thank the staff of the beam line for their assistance. The EXAFS data were analyzed with the software XDAP.[20]

Supporting Information Available: Thermogravimetry data characterizing the zeolite NaY used in the synthesis (PDF). This material is available free of charge via the Internet at http://pubs.acs.org.

References and Notes

(1) Ichikawa, M. *Adv. Catal.* **1992**, *38*, 283.

(2) Kawi, S.; Gates, B. C. In *Clusters and Colloids—from Theory to Applications*; Schmid, G., Ed.; VCH: Weinheim, Germany, 1994; p 299.

(3) (a) Malatest, L.; Caglio, G.; Angoletta, M. *Inorg. Synth.* **1971**, *13*, 95. (b) Beneke, M.; Brabec, L.; Jeager, N.; Novakova, J.; Schulz-Ekloff, G. *J. Mol. Catal. A* **2000**, *157*, 151.

(4) Li, F.; Gates, B. C. *J. Phys. Chem. B* **2003**, *107*, 11589.

(5) Kawi, S.; Chang, J.-R.; Gates, B. C. *J. Am. Chem. Soc.* **1993**, *115*, 4830.

(6) Kawi, S.; Gates, B. C. *Catal. Lett.* **1991**, *10*, 263. The spectra of metal carbonyls in zeolites, including ours, show broadening of the ν_{CO} peaks, consistent with polar interactions of the carbonyl groups with polar groups, such as exchange ions, at various positions in the zeolite (Kawi, S.; Chang, J.-R.; Gates, B. C. *J. Phys. Chem.* **1993**, *97*, 5375).

(7) Alexeev, O.; Panjabi, G.; Gates, B. C. *J. Catal.* **1998**, *173*, 196.

(8) Zhao, A.; Gates, B. C. *J. Am. Chem. Soc.* **1996**, *118*, 2458.

(9) Weber, W. A.; Gates, B. C. *J. Phys. Chem. B* **1997**, *101*, 10423.

(10) Kawi, S.; Chang, J.-R.; Gates, B. C. *J. Phys. Chem.* **1993**, *97*, 10599.

(11) Maloney, S. D.; Kelley, M. J.; Koningsberger, D. C.; Gates, B. C. *J. Phys. Chem.* **1991**, *95*, 9406.

(12) Wyckoff, R. W. G. *Crystal Structures*, 2nd ed.; Wiley: New York, 1963; Vol. 1, p 10.

(13) Trömel, M.; Lupprich, E. *Z. Anorg. Allg. Chem.* **1975**, *414*, 160.

(14) Duivenvoorden, F. B. M.; Koningsberger, D. C.; Uh, Y. S.; Gates, B. C. *J. Am. Chem. Soc.* **1986**, *108*, 6254.

(15) Churchill, M. R.; Hutchinson, J. P. *Inorg. Chem.* **1978**, *17*, 3528.

(16) Koningsberger, D. C. In *Synchrotron Techniques in Interfacial Electrochemistry*; Melendres, C. A., Tadjeddine, A., Eds.; Kluwer: Dordrecht, The Netherlands, 1994; p 181.

(17) Alexeev, O. S.; Graham, G. W.; Shelef, M.; Adams, R. D.; Gates, B. C. *J. Phys. Chem. B* **2002**, *106*, 4697.

(18) Hanlan, L. A.; Ozin, G. A. *J. Am. Chem. Soc.* **1974**, *96*, 6324.

(19) Shannon, R. D.; Staley, R. H.; Vega, A. J.; Fischer, R. X.; Baur, W. H.; Auroux, A. *J. Phys. Chem.* **1989**, *93*, 2019.

(20) Vaarkamp, M. *Catal. Today* **1998**, *39*, 271.

(21) Vaarkamp, M.; Linders, J. C.; Koningsberger, D. C. *Physica B (Amsterdam)* **1995**, *208*, *209*, 159.

(22) Koningsberger, D. C., Prins, R., Eds. *X-ray Absorption: Principles, Applications, Techniques of EXAFS, SEXAFS, and XANES*; Wiley: New York, 1988; p 395.

(23) There is a small peak in the spectrum of Figure 3g at 1818 cm^{-1}. It is slightly more intense than that of Kawi.[6] The difference is suggested to be a result of the fact that he stopped collecting IR spectra after 3.5 h of CO treatment at 40 °C, and Figure 3g was recorded after 20 h of CO treatment at 40 °C.

(24) This peak at 1818 cm^{-1} of Figure 3g calls for interpretation: One possibility is that some tetrairidium carbonyl clusters might have been disordered (the disordered bridging form of the cluster might give this band).[15] Another possibility to be considered is that it may be the bridging band of a species such as $Ir_2(CO)_8$ or $Ir_6(CO)_{16}$; however, there are no other ν_{CO} bands characteristic of $Ir_2(CO)_8$ (such as those at 2096, 2055, and 2053 cm^{-1}) or of $Ir_6(CO)_{16}$ (such as those at 2129, 2097, and 2084 cm^{-1}), and so this possibility is discounted. Hanlan et al.[18] provided IR evidence attributed to an unusual isomer of $Ir_4(CO)_{12}$ with bridging ligands (ν_{CO} = 2068 s, 2035 ms, and 1869 m cm^{-1}), pointing out that at room temperature $Ir_4(CO)_{12}$ slowly disproportionates to give $Ir_6(CO)_{16}$;[18] thus, we do not rule out this possibility.

(25) Cariati, E.; Roberto, D.; Ugo, R.; Lucenti, E. *Chem. Rev.* **2003**, *103*, 3707.

(26) Turkevich, J. *Catal. Rev.* **1967**, *1*, 1.

(27) Pergola, R. D.; Garlaschelli, L.; Martinengo, S. *Inorg. Synth.* **1990**, *28*, 245.

(28) Garlaschelli, L.; Martinengo, S.; Bellon, P. L.; Demartin, F.; Manassero, M.; Chiang, M. Y.; Wei, C. Y.; Bau, R. *J. Am. Chem. Soc.* **1984**, *106*, 6664.

(29) Hanlan, A. J. L.; Ozin, G. A. *J. Organomet. Chem.* **1979**, *179*, 57.

(30) Whyman, R. *J. Chem. Soc., Dalton Trans.* **1972**, 2294.

(31) Whyman, R. *J. Chem. Soc., Dalton Trans.* **1972**, 1375.

(32) Whyman, R. *J. Chem. Soc., Chem. Commun.* **1970**, 1194.